Journal of Enzyme Inhibition and Medicinal Chemistry

http://informahealthcare.com/enz
ISSN: 1475-6366 (print), 1475-6374 (electronic)

J Enzyme Inhib Med Chem, Early Online: 1–8
 DOI: 10.3109/14756366.2014.959947

informa
healthcare

RESEARCH ARTICLE

Preparation, anticholinesterase activity, and docking study of new 2-butenediamide and oxalamide derivatives

Kadir Ozden Yerdelen[1], Mehmet Koca[1], Zeynep Kasap[1], and Baris Anil[2]

[1]Department of Pharmaceutical Chemistry and [2]Department of Organic Chemistry, Faculty of Pharmacy, Ataturk University, Erzurum, Turkey

Abstract

Several new oxalamide and 2-butenediamide derivatives have been designed, synthesized and evaluated as the acetyl- and butyryl-cholinesterase inhibitors for Alzheimer's disease. The enzyme inhibitory activity of the synthesized compounds was measured using Ellman's colorimetric method. It was revealed that compound **1a** (*N,N′-bis-(4-chloro-benzyl)-N,N′-diphenyl-oxalamide*) showed maximum activity against BuChE with a half maximal inhibitory concentration (IC_{50}) = 1.86 μM and compound **2a** (*but-2-enedioic acid bis-[(4-chloro-benzyl)-phenyl-amide]*) exhibited optimum AChE (IC_{50} = 1.51 μM) inhibition with a high-selectivity index. To better understand the enzyme–inhibitor interaction of the most active compounds towards cholinesterase, molecular modelling studies were carried out. Docking simulations revealed that inhibitors **1a** and **2a** targeted both the catalytic active site and the peripheral anionic site of 1ACJ and 1P0I.

Keywords

2-butenediamide, Alzheimer, metal chelation, molecular modelling, oxalamide

History

Received 6 August 2014
Revised 27 August 2014
Accepted 27 August 2014
Published online 27 November 2014

Introduction

Dementia is a loss of brain function that occurs with certain diseases. Alzheimer's disease (AD) is one form of dementia that gradually gets worse over time and it can cause symptoms such as the loss of memory, learning and language skills[1–4]. The progression and definite causes of AD are still mostly unknown, but the most common hypotheses to have been put forward are based on causative factors and include the cholinergic, amyloid, tau and metal hypotheses[5]. Standard medical treatment for AD includes cholinesterase inhibitors (ChEIs) and partial N-methyl-D-aspartate (NMDA) antagonists[6,7]. The cholinergic hypothesis is one of the oldest and most popular hypotheses outlining the pathogenesis of AD. According to the cholinergic hypothesis, the main approach of the current pharmacotherapy for AD is to increase the levels of acetylcholine (ACh) through the inhibition of cholinesterase enzymes (ChEs)[8–10]. Acetylcholinesterase (AChE) and butyryl-cholinesterase (BuChE), which are located in the central nervous system (CNS), are able to hydrolyse the neurotransmitter ACh[11]. Studies have shown that AD is defined by the rapid loss of AChE activity in the early stages of the disease, along with an increasing ratio of AChE as the disease progresses[12,13]. Furthermore, BuChE has been found to be capable of compensating for the missing AChE catalytic functions in the synaptic cleft, and its activity increases by 30–60% during AD[14–17]. Due to the role of BuChE in the hydrolysis of ACh, the inhibition of both ChEs using a dual inhibitor should result in increased levels of ACh in the brain, which provide more successful clinical efficacy of AD[18,19].

Address for correspondence: Kadir Ozden Yerdelen, Assist. Prof., Department of Pharmaceutical Chemistry, Faculty of Pharmacy, Ataturk University, 25240 Erzurum, Turkey. Tel: +90-442-2315220. Fax: +90-442-2360962. E-mail: dadasozden@gmail.com

High levels of metals like mercury cause severe and fatal neurologic diseases, as well as learning and memory problems and movement disorders[20]. However, some metals are essential for brain function. Imbalances in the level and distribution of these metals in the brain, especially zinc, copper and iron, may play a role in diseases like AD (this pertains to the so-called ''metal hypothesis'')[21]. The level of metal ions (Fe^{2+}, Cu^{2+} and Zn^{2+}) in AD patients is 3–7 times higher than it is in healthy individuals[22]. For example, abnormally high levels of iron are often found in the brains of people who die of Alzheimer's disease[23]. In addition, copper, iron and zinc are all associated with abnormal clumps of brain proteins (plaques), which are a hallmark of Alzheimer's disease[24–26].

The aim of this study was to synthesize and develop new oxalamide and 2-butenediamide derivatives as potential anticholinesterase and chelator agents.

Materials and methods

Experimental

The melting points were measured on an Electrothermal 9100 (Thomas Hoover, USA) melting-point apparatus. The ^1H and ^{13}C NMR spectra were recorded with a Bruker FT-400(100) MHz (Rheinstetten, Germany) spectrometer using deuterated chloroform ($CDCl_3$) as the solvent. Mass spectra were recorded on an Agilent 1200 (Waldbronn, Germany) mass spectrometer at 10 eV. Benzaniline compounds were synthesized with a CEM 3100 (Matthews, NC) microwave oven. Reaction progress and product mixtures were routinely checked by thin-layer chromatography (TLC) on Merck SilicaGel F254 (Darmstadt, Germany) aluminium plates. The chemical reagents and solvents used in this study were purchased from Merck (Darmstadt, Germany) or Sigma Aldrich (Munich, Germany).

A general procedure for the synthesis of oxalamide compounds (1a–h)

(4-Chloro-benzyl)-(4-substituted-phenyl)-amine derivatives were prepared with microwave (150 W, 120 °C) irradiation under solvent-free phase transfer catalysis conditions. To synthesise the oxalamide derivatives, a mixture of (4-chloro-benzyl)-(4-substituted-phenyl)-amine (1.4 mmol), triethylamine (1.4 mmol) and oxalyl chloride (0.7 mmol) in tetrahydrofuran (10 ml) was stirred at room temperature for 12 h. The reaction mixture was quenched with 15 ml of distilled water, and the aqueous phase was extracted with two portions of CH_2Cl_2. The combined organic layers were dried over Na_2SO_4, filtered and concentrated. The obtained solid was recrystallized from ethanol. The synthesis pathway is shown in Scheme 1.

N,N′-Bis-(4-chloro-benzyl)-N,N′-diphenyl-oxalamide (***1a***) was obtained from (4-chloro-benzyl)-phenyl-amine according to the general procedure as white solid. Yield 68%; m.p. 102–105 °C. The crude compound was recrystallized from ethanol. ^{1}H-NMR (400 MHz, $CDCl_3$) δ: 4.62 (s, 4H, 2× CH_2-N), 6.66 (d, 4H, $J = 8.40$ Hz, Ar-H), 6.87 (d, 4H, $J = 8.56$ Hz, Ar-H), 7.06 (d, 4H, $J = 8.40$ Hz, Ar-H), 7.31–7.27 (m, 2H, Ar-H), 7.37–7.35 (m, 2H, Ar-H). ^{13}C-NMR (100 MHz, $CDCl_3$) δ: 51.37 (CH_2–N), 128.50, 128.60, 129.14, 129, 17 129.54, 133.23, 134.81, 139.23, 164.34 (C=O). ESI-MS *m/z* [M+H] 489.4.

N,N′-Bis-(4-chloro-benzyl)-N,N′-di-p-tolyl-oxalamide (***1b***) was obtained from (4-chloro-benzyl)-*p*-tolyl-amine according to the general procedure as white solid. Yield 64%; m.p. 175–178 °C. The crude compound was recrystallized from ethanol. ^{1}H-NMR (400 MHz, $CDCl_3$) δ: 2.45 (s, 6H, 2× Ar-CH_3), 4.58 (s, 4H, 2× CH_2–N), 6.69 (d, 4H, $J = 8.36$ Hz, Ar-H), 6.75 (d, 4H, $J = 8.28$ Hz, Ar-H), 7.05 (d, 4H, $J = 8.36$ Hz, Ar-H), 7.07 (d, 4H, $J = 8.28$ Hz, Ar-H). ^{13}C-NMR (100 MHz, $CDCl_3$) δ: 21.19 (Ar-CH_3), 51.41 (CH_2–N), 128.37, 129.61, 129.71, 133.13, 135.03, 136.70, 138.65, 164.52 (C=O). ESI-MS *m/z* [M+H] 517.5.

N,N′-Bis-(4-chloro-benzyl)-N,N′-bis-(4-ethyl-phenyl)-oxalamide (***1c***) was obtained from (4-chloro-benzyl)-(4-ethyl-phenyl)-amine according to the general procedure as white solid. Yield 59%; m.p. 192–195 °C. The crude compound was recrystallized from ethanol. ^{1}H-NMR (400 MHz, $CDCl_3$) δ: 1.28–1.25 (t, 6H, 2× CH_2–CH_3), 2.72–2.66 (q, 4H, 2× CH_2–CH_3), 4.59 (s, 4H 2× CH_2–N), 6.71 (d, 4H, $J = 8.40$ Hz, Ar-H), 6.77 (d, 4H, $J = 8.32$ Hz, Ar-H), 7.05 (d, 4H, $J = 8.40$ Hz, Ar-H), 7.09 (d, 4H, $J = 8.30$ Hz, Ar-H). ^{13}C-NMR (100 MHz, $CDCl_3$) δ: 15.18 (CH_2–CH_3), 28.41 (CH_2–CH_3), 51.46 (CH_2–N), 128.36, 128.40, 129.67, 129.71, 133.12, 135.07, 136.85, 144.79, 164.55 (C=O). ESI-MS *m/z* [M+H] 545.7.

N,N′-Bis-(4-chloro-benzyl)-N,N′-bis-(4-methoxy-phenyl)-oxalamide (***1d***) was obtained from (4-chloro-benzyl)-(4-methoxy-phenyl)-amine according to the general procedure as white solid. Yield 44%; m.p. 187–190 °C. The crude compound was recrystallized from ethanol. ^{1}H-NMR (400 MHz, $CDCl_3$) δ: 3.83 (s, 6H, 2× OCH_3), 4.58 (s, 4H, 2× CH_2–N), 6.66 (d, 4H, $J = 8.30$ Hz, Ar-H), 6.77 (d, 4H, $J = 9.30$ Hz, Ar-H), 6.81 (d, 4H, $J = 9.28$ Hz, Ar-H), 7.06 (d, 4H, $J = 8.30$ Hz, Ar-H). ^{13}C-NMR (100 MHz, $CDCl_3$) δ: 51.40 (CH_2-N), 51.42 (OCH_3), 114.02, 128.43, 129.73, 130.08, 131.87, 133.18, 135.10, 159.59, 164.73 (C=O). ESI-MS *m/z* [M + H] 549.3.

N,N′-Bis-(4-chloro-benzyl)-N,N′-bis-(4-ethoxy-phenyl)-oxalamide (***1e***) was obtained from (4-chloro-benzyl)-(4-ethoxy-phenyl)-amine according to the general procedure as white solid. Yield 26%; m.p. 137–140 °C. The crude compound was recrystallized from ethanol. ^{1}H-NMR (400 MHz, $CDCl_3$) δ: 1.49–1.46 (t, 6H, 2× OCH_2–CH_3), 4.05–4.00 (q, 4H, 2× OCH_2CH_3),

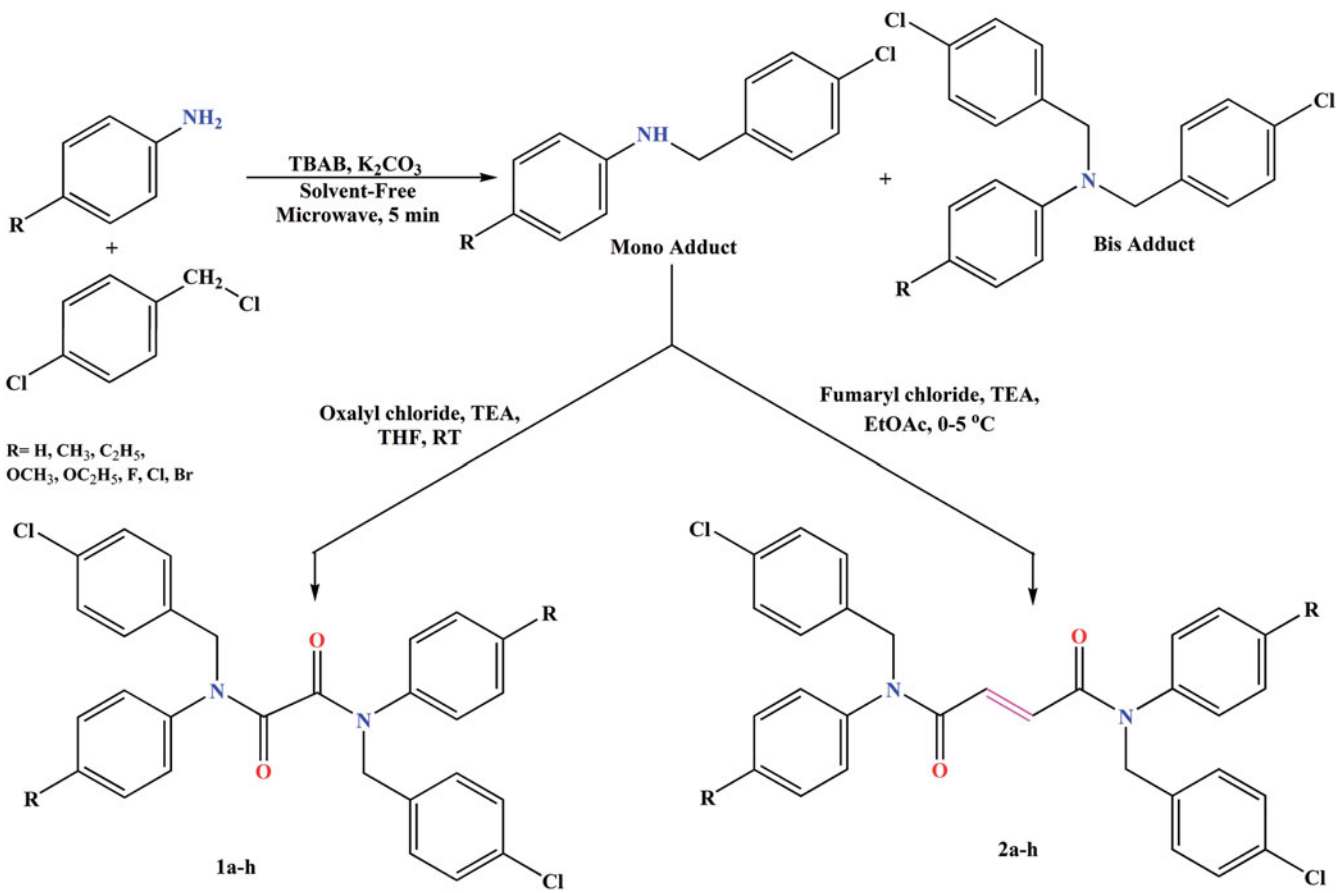

Scheme 1. Synthesis of the target compounds **1a–h** and **2a–h**.

4.57 (s, 4H, 2× CH_2-N), 6.65 (d, 4H, $J = 8.28$ Hz, Ar-H), 6.75 (d, 4H, $J = 9.24$ Hz, Ar-H), 6.78 (d, 4H, $J = 9.32$ Hz, Ar-H), 7.06 (d, 4H, $J = 8.32$ Hz, Ar-H). ^{13}C-NMR (100 MHz, $CDCl_3$) δ: 14.81 (OCH_2CH_3), 51.40 (CH_2–N), 63.74 (OCH_2CH_3), 114.41, 128.42, 129.69, 130.04, 131.68, 133.13, 135.14, 159.64, 164.82 (C=O). ESI-MS *m/z* [M+H] 577.5.

*N,N′-Bis-(4-chloro-benzyl)-N,N′-bis-(4-fluoro-phenyl)-oxalamide (**1f**)* was obtained from (4-chloro-benzyl)-(4-fluoro-phenyl)-amine according to the general procedure as white solid. Yield 52%; m.p. 147–150 °C. The crude compound was recrystallized from ethanol. ^{1}H-NMR (400 MHz, $CDCl_3$) δ: 4.59 (s, 4H, 2× CH_2-N), 6.85 (d, 4H, $J = 8.88$ Hz, Ar-H), 6.86 (d, 4H, $J = 8.88$ Hz, Ar-H), 6.98 (d, 4H, $J = 8.20$ Hz, Ar-H), 7.12 (d, 4H, $J = 8.36$ Hz, Ar-H). ^{13}C-NMR (100 MHz, $CDCl_3$) δ: 51.37 (CH_2–N), 115.98, 116.20, 128.66, 129.68, 130.59, 130.67, 133.67, 134.46 (C-F), 164.12 (C=O). ESI-MS *m/z* [M+H] 525.3.

*N,N′-Bis-(4-chloro-benzyl)-N,N′-bis-(4-chloro-phenyl)-oxalamide (**1g**)* was obtained from (4-chloro-benzyl)-(4-chloro-phenyl)-amine according to the general procedure as white solid. Yield 42%; m.p. 182–185 °C. The crude compound was recrystallized from ethanol. ^{1}H-NMR (400 MHz, $CDCl_3$) δ: 4.59 (s, 4H, 2× CH_2–N), 6.69 (d, 4H, $J = 8.40$ Hz, Ar-H), 6.80 (d, 4H, $J = 8.68$ Hz, Ar-H), 7.14 (d, 4H, $J = 8.40$ Hz, Ar-H), 7.27 (d, 4H, $J = 8.84$ Hz, Ar-H). ^{13}C-NMR (100 MHz, $CDCl_3$) δ: 51.31 (CH_2–N), 128.73, 129.40, 129.66, 129.95, 133.77, 134.33, 134.91, 137.53, 163.89 (C=O). ESI-MS *m/z* [M + H] 557.4.

*N,N′-Bis-(4-bromo-phenyl)-N,N′-bis-(4-chloro-benzyl)-oxalamide (**1h**)* was obtained from (4-bromo-phenyl)-(4-chloro-benzyl)-amine according to the general procedure as white solid. Yield 66%; m.p. 217–220 °C. The crude compound was recrystallized from ethanol. ^{1}H-NMR (400 MHz, $CDCl_3$) δ: 4.59 (s, 4H, 2× CH_2–N), 6.69 (d, 4H, $J = 8.40$ Hz, Ar-H), 6.73 (d, 4H, $J = 8.64$ Hz, Ar-H), 7.16 (d, 4H, $J = 8.40$ Hz, Ar-H), 7.42 (d, 4H, $J = 8.64$ Hz, Ar-H). ^{13}C-NMR (100 MHz, $CDCl_3$) δ: 51.28 (CH_2–N), 128.78, 128.82, 129.65, 132.42, 133.78, 134.32, 138.05, 163.80 (C=O). ESI-MS *m/z* [M + H] 645.7.

General procedure for the synthesis of 2-butenediamide derivatives (2a–h)

The mixture of (4-chloro-benzyl)-(4-substituted-phenyl)-amine (1.4 mmol), triethylamine (TEA) (1.4 mmol) and dry ethylacetate (5 ml) was cooled with an ice bath to 0–5 °C, and fumaryl chloride (0.65 mmol) in 5 ml dry ethylacetate was added dropwise by syringe over 30 min. The reaction mixture was then stirred at room temperature for 12 h. The reaction mixture was quenched with 50 ml of water, and the aqueous phase was extracted with two portions of CH_2Cl_2. The combined organic layers were dried over $MgSO_4$, filtered and concentrated by rotary evaporation. The target compounds were recrystallized from ethanol. The synthesis procedure is described in our previously reported study[27].

*But-2-enedioic acid bis-[(4-chloro-benzyl)-phenyl-amide] (**2a**)* was obtained from (4-chloro-benzyl)-phenyl-amine according to general procedure as bright yellow. Yield 52%; m.p. 203–206 °C. The crude compound was recrystallized from ethanol. ^{1}H-NMR (400 MHz, $CDCl_3$) δ: 4.85 (s, 4H, 2× CH_2–N), 6.86 (s, 2H, fumaryl CH=CH), 6.96 (d, 4H, $J = 7.88$ Hz, Ar-H), 7.07 (d, 4H, $J = 8.32$ Hz, Ar-H), 7.19 (d, 4H, $J = 8.32$ Hz, Ar-H), 7.35 (d, 4H, $J = 7.88$ Hz, Ar-H). ^{13}C-NMR (100 MHz, $CDCl_3$) δ: 52.90 (CH_2–N), 128.01, 128.43, 128.61, 129.87, 130.09, 132.06 (CH=CH), 133.40, 135.41, 140.97, 164.34 (C=O). ESI-MS *m/z* [M + H] 515.7.

*But-2-enedioic acid bis-[(4-chloro-benzyl)-p-tolyl-amide] (**2b**)* was obtained from (4-chloro-benzyl)-*p*-tolyl-amine according to general procedure as white solid. Yield 45%; m.p. 201–204 °C. The crude compound was recrystallized from ethanol. ^{1}H-NMR (400 MHz, $CDCl_3$) δ: 2.35 (s, 6H, 2× Ar-CH_3), 4.83 (s, 4H, 2× CH_2–N), 6.82 (d, 4H, $J = 8.20$ Hz, Ar-H), 6.86 (s, 2H, fumaryl CH=CH), 7.08 (d, 4H, $J = 8.40$ Hz, Ar-H), 7.13 (d, 4H, $J = 8.08$ Hz, Ar-H), 7.18 (d, 4H, $J = 8.02$ Hz, Ar-H). ^{13}C-NMR (100 MHz, $CDCl_3$) δ: 21.11 (Ar-CH_3), 52.87 (CH_2–N), 127.75, 128.56, 130.12, 130.47, 131.97 (CH=CH), 133.32, 135.54, 138.32, 138.41, 164.50 (C=O). ESI-MS *m/z* [M + H] 543.2.

*But-2-enedioic acid bis-[(4-chloro-benzyl)-(4-ethyl-phenyl)-amide] (**2c**)* was obtained from (4-chloro-benzyl)-(4-ethyl-phenyl)-amine according to general procedure as bright yellow. Yield 55%; m.p. 194–197 °C. The crude compound was recrystallized from ethanol. ^{1}H-NMR (400 MHz, $CDCl_3$) δ: 1.27–1.23 (t, 6H, 2× CH_2–CH_3), 2.68–2.62 (q, 4H, 2× CH_2–CH_3), 4.83 (s, 4H 2× CH_2–N), 6.86 (d, 4H, $J = 8.24$ Hz, Ar-H), 6.89 (s, 2H, fumaryl CH=CH), 7.09 (d, 4H, $J = 8.40$ Hz, Ar-H), 7.16 (d, 4H, $J = 8.24$ Hz, Ar-H), 7.19 (d, 4H, $J = 8.40$ Hz, Ar-H). ^{13}C-NMR (100 MHz, $CDCl_3$) δ: 24.35 (CH_2–CH_3), 29.89 (CH_2–CH_3), 52.39 (CH_2–N), 127.91, 128.36, 129.67, 129.71, 134.42 (CH=CH), 135.07, 136.45, 143.85, 163.35 (C=O). ESI-MS *m/z* [M + H] 571.4.

*But-2-enedioic acid bis-[(4-chloro-benzyl)-(4-methoxy-phenyl)-amide] (**2d**)* was obtained from (4-chloro-benzyl)-(4-methoxy-phenyl)-amine according to general procedure as bright yellow solid. Yield 52%; m.p. 160–163 °C. The crude compound was recrystallized from ethanol. ^{1}H-NMR (400 MHz, $CDCl_3$) δ: 3.80 (s, 6H, 2× OCH_3), 4.81 (s, 4H, 2× CH_2-N), 6.84 (s, 2H, fumaryl CH=CH), 6.85 (br s, 8H, Ar-H), 7.08 (d, 4H, $J = 8.24$ Hz, Ar-H), 7.19 (d, 4H, $J = 8.28$ Hz, Ar-H). ^{13}C-NMR (100 MHz, $CDCl_3$) δ: 52.95 (CH_2–N), 55.44 (OCH_3), 114.97, 128.58, 129.17, 130.24, 131.94 (CH=CH), 133.35, 133.52, 135.51, 159.29, 164.64 (C=O). ESI-MS *m/z* [M + H] 575.6.

*But-2-enedioic acid bis-[(4-chloro-benzyl)-(4-ethoxy-phenyl)-amide] (**2e**)* was obtained from (4-chloro-benzyl)-(4-ethoxy-phenyl)-amine according to general procedure as white solid. Yield 45%; m.p. 167–170 °C. The crude compound was recrystallized from ethanol. ^{1}H-NMR (400 MHz, $CDCl_3$) δ: 1.44–1.41 (t, 6H, 2× OCH_2–CH_3), 4.04–3.98 (q, 4H, 2× OCH_2CH_3), 4.80 (s, 4H, 2× CH_2–N), 6.82 (s, 2H, fumaryl CH=CH), 7.07 (d, 4H, $J = 6.56$ Hz, Ar-H), 7.08 (d, 4H, $J = 6.64$ Hz, Ar-H), 7.19 (d, 4H, $J = 6.52$ Hz, Ar-H), 7.20 (d, 4H, $J = 6.48$ Hz, Ar-H). ^{13}C-NMR (100 MHz, $CDCl_3$) δ: 14.80 (OCH_2CH_3), 52.94 (CH_2-N), 63.70 (OCH_2CH_3), 115.39, 128.56, 129.14, 130.25, 131.93 (CH=CH), 133.34, 135.54, 158.73, 165.21 (C=O). ESI-MS *m/z* [M + H] 603.5.

*But-2-enedioic acid bis-[(4-chloro-benzyl)-(4-fluoro-phenyl)-amide] (**2f**)* was obtained from (4-chloro-benzyl)-(4-fluoro-phenyl)-amine according to general procedure as white solid. Yield 27%; m.p. 194–197 °C. The crude compound was recrystallized from ethanol. ^{1}H-NMR (400 MHz, $CDCl_3$) δ: 4.82 (s, 4H, 2× CH_2-N), 6.82 (s, 2H, fumaryl CH=CH), 6.92 (d, 4H, $J = 8.84$ Hz, Ar-H), 7.03 (d, 4H, $J = 8.24$ Hz, Ar-H), 7.06 (d, 4H, $J = 8.36$ Hz, Ar-H), 7.21 (d, 4H, $J = 8.40$ Hz, Ar-H). ^{13}C-NMR (100 MHz, $CDCl_3$) δ: 52.92 (CH_2–N), 128.72, 129.92, 130.14, 130.17, 130.20, 131.99 (CH=CH), 133.63, 135.07 (C–F), 164.20 (C=O). ESI-MS *m/z* [M + H] 551.2.

*But-2-enedioic acid bis-[(4-chloro-benzyl)-(4-chloro-phenyl)-amide] (**2g**)* was obtained from (4-chloro-benzyl)-(4-chloro-phenyl)-amine according to general procedure as white solid. Yield 57%; m.p. 216–219 °C. The crude compound was recrystallized from ethanol. ^{1}H-NMR (400 MHz, $CDCl_3$) δ: 4.83 (s, 4H, 2× CH_2–N), 6.82 (s, 2H, fumaryl CH=CH), 6.89 (d, 4H, $J = 8.60$ Hz, Ar-H), 7.07 (d, 4H, $J = 8.31$ Hz, Ar-H), 7.21 (d, 4H, $J = 8.30$ Hz, Ar-H), 7.33 (d, 4H, $J = 8.60$ Hz, Ar-H). ^{13}C-NMR (100 MHz, $CDCl_3$) δ: 52.83 (CH_2-N), 128.76, 129.34, 130.15, 132,06 (CH=CH), 133.68, 134.96, 139.31, 164.02 (C=O). ESI-MS *m/z* [M + H] 583.4.

*But-2-enedioic acid bis-[(4-bromo-phenyl)-(4-chloro-benzyl)-amide] (**2h**)* was obtained from (4-bromo-phenyl)-(4-chloro-benzyl)-amine according to general procedure as bright yellow. Yield 27%; m.p. 213–216 °C. The crude compound was recrystallized from ethanol. ^{1}H-NMR (400 MHz, $CDCl_3$) δ: 4.83 (s, 4H, 2× CH_2–N), 6.82 (d, 4H, $J = 8.52$ Hz, Ar-H), 6.83 (s, 2H, fumaryl CH=CH), 7.07 (d, 4H, $J = 8.40$ Hz, Ar-H), 7.21 (d, 4H, $J = 8.36$ Hz, Ar-H), 7.48 (d, 4H, $J = 8.60$ Hz, Ar-H). ^{13}C-NMR (100 MHz, $CDCl_3$) δ: 52.79 (CH_2–N), 122.55, 128.77, 129.64, 130.13, 132.07 (CH=CH), 133.69, 134.94, 139.83, 163.95 (C=O). ESI-MS *m/z* [M + H] 670.8.

Inhibition studies on AChE and BuChE

AChE, BuChE, 5,5-dithiobis-(2-nitrobenzoic acid) DTNB, acetylthiocholine iodide (ATCI) and butyrylthiocholine iodide (BTCI) were purchased from Sigma Aldrich. The inhibitory activities of the AChE and BuChE test compounds were evaluated using Ellman's colorimetric method[28] with some modifications using commercially available neostigmine bromide[11] and ambenonium dichloride[29] as the reference compounds. The test compounds were dissolved in dimethylsulfoxide and then diluted in a 50-mM Tris buffer (pH 8.0) to provide a final concentration range. In a 96-well plate, the assay medium in each well consisted of 50 µl of a Tris buffer, 125 µl of 3 mM DTNB (Ellman's reagent), 25 µl of 0.2 U/ml enzyme (AChE or BuChE) and a 15-mM substrate (ATCI or BTCI). The assay mixture containing the enzyme, buffer, DTNB and 25 µl of the inhibitor compound was preincubated for 15 min at 37 °C before the substrate was added to begin the reaction. Neostigmine bromide, ambenonium dichloride and all test compounds were prepared at 11 different concentrations: 0.09, 0.195, 0.39, 0.78, 1.56, 3.13, 6.25, 12.5, 25, 50 and 100 µg/ml. The absorbance of the reaction mixture was then measured three times at 412 nm every 45 s using a microplate reader (Bio-Tek ELx800, USA). The results are presented as mean ± standard errors of the experiment. The IC_{50} values of the compounds showing percentage inhibition, the measurements and the calculations were evaluated by non-linear regression analysis using GraphPad Prism software.

Spectrophotometric measurement of chelation capacity

The ability of metal chelation was determined by measuring the formation of metal complexes in dimethylsulfoxide (DMSO) at room temperature using a UV–visible spectrophotometer (Thermo Electron Heλios) with a wavelength ranging from 190 to 380 nm[30,31]. The UV absorption of test compounds **1a** and **2a**, in the absence or presence of $CuSO_4$, $FeSO_4$ and $ZnSO_4$, was recorded in a 1-cm quartz cuvette after 20 min at room temperature. The final volume of the reaction mixture was 3 ml, and the final concentrations of the test compounds and metals were 100 µM.

Docking procedure

The docking study was performed using Surflex-Dock in Sybyl-X 2.0 by Tripos Associates. 3D structures of compounds **1a** and **2a** were constructed using the Sybyl sketcher module. The structures were minimized using the steepest descent conjugated gradient method until the gradient was 0.001 kcal/mol and max iterations: 1000 with the Tripos force field with the Gasteiger–Huckel charge. The simulation system was built on the crystal structures of 1ACJ and 1P0I, which were obtained from the Protein Data Bank. At the commencement of docking, all the water and ligands were removed and the random hydrogen atoms were added. Docking calculations using Surflex-Dock for 1ACJ and 1P0I were performed through protomol generation by ligand. The parameters used were threshold 0.5 and bloat 0.

Result and discussion

Chemistry

Compounds **1a–h** were synthesized by the reaction of oxalyl chloride with *para*-(4-chloro-benzyl)-(4-substituted-phenyl)-amines in tetrahydrofuran in the presence of triethylamine with moderate to good yields (26–68%). 2-Butenediamide derivatives (**2a–h**) were obtained in moderate yields (27–57%). The obtained spectroscopic data are in accordance with the predicted structures. The synthesis scheme of the compounds is presented in Scheme 1. In the proton nuclear magnetic resonance (^{1}H-NMR) spectra, the resonance signals of ethylene bridge protons are registered as singlets in the range of 6.82 to 6.89 ppm for compounds **2a–f**. The signals for aromatic protons were showed in the range of δ 6.65–7.42 and δ 6.82–7.48 ppm for compounds **1a–h** and **2a–h**, respectively. The N-CH_2 protons appeared at δ 4.57–4.62 ppm for compounds **1a–h** and δ 4.80–4.85 ppm for compounds **2a–h**. The carbon nuclear magnetic resonance (^{13}C-NMR) spectrum shows characteristic carbon resonance frequencies of carbonyl atoms in the range of 163.80–164.82 ppm for compounds **1a–h** and 163.35–165.21 ppm for compounds **2a–h**. The aromatic carbons appeared at δ 114.97–159.64 ppm and N–CH_2 groups appeared at δ 51.28–52.90 ppm. In the positive electron impact (EI) mass spectra, the molecular ion peaks [M + H] show that the predicted compound has formed. Spectral data of the compounds are documented in Supplementary file.

In vitro cholinesterase enzymes inhibitory activity

The inhibitory activity of the compounds against AChE and BuChE was measured according to the colorimetric assay of Ellman[28]. Neostigmine and ambenonium were used as the reference compounds. The IC_{50} values of all tested compounds and their selectivity index for AChE are summarized in Table 1. In general, butenediamide derivatives **2a–h** showed moderate to good inhibitory activity on AChE with micromolar concentrations. The non-substituted compound among the butenediamide derivatives, **2a** ($IC_{50} = 1.51$ µM), showed the most potent inhibitory activity against AChE, being 4.47- and 2.69-fold stronger than the reference compounds neostigmine bromide ($IC_{50} = 6.76$ µM) and ambenonium dichloride ($IC_{50} = 4.07$ µM), respectively. The other compound in the series, **2f**, was found to be the second most powerful compound, with an IC_{50} value of 2.47 µM. In addition, the most potent compounds, **2a** and **2f**, were found to be more selective inhibitors on AChE than the other compounds with 62.11 and 40.48 selectivity index (SI) values, respectively. At the same time, compounds **2g** and **2h** showed similar activity to the reference compounds. Compounds **2b** and **2c** were found to have moderate inhibitory activity on AChE and BuChE, with an IC_{50} of 87.09 and 26.30 µM, respectively. A similar situation was seen on BuChE inhibition with IC_{50} values of 11.22 and 35.48 µM for the same compounds (**2b** and **2c**). Compound **2g** exhibited the strongest inhibition to BuChE, with an IC_{50} value of 7.07 µM. In addition, compound **2g** exhibited 2.04-fold stronger inhibition against BuChE than the reference compound neostigmine bromide ($IC_{50} = 14.45$ µM).

On the other hand, **1a** exhibited the strongest inhibition to BuChE, with an IC_{50} value of 1.86 µM, which was 7.76- and 3.23-fold more potent than those of neostigmine ($IC_{50} = 14.45$ µM) and ambenonium ($IC_{50} = 6.02$ µM). In addition, compound **1a** had a high level of BuChE inhibitor selectivity. Compound **1b** was found to have moderate inhibitory activity on BuChE, with an IC_{50} of 72.02 µM. The other oxalamide derivatives did not exhibit

inhibitory activity against both ChEs (Table 1). These compounds in the series were considered to be inactive since their IC_{50} values were more than 100 μM.

From the IC_{50} values, the butenediamide derivatives (except for **2d** and **2e**) seemed to be more effective than the oxalamide derivatives on AChE inhibition due to the ethylene bridge for the linker between the two carbonyl groups. This finding suggests that acetylcholinesterase's inhibitory activity is strongly dependent on the presence of an ethylene moiety in the inhibitors. In our previously reported study, the results of anticholinesterase activity showed that the α,β-unsaturated moiety contributed to the interaction with cholinesterase enzymes[27].

Table 1. Anticholinesterase activity of IC_{50} (μM) and selectivity of compounds **1a–h** and **2a–h** on AChE and BuChE.

			IC_{50} (μM)		
Compounds	R^1	R^2	AChE[a]	BuChE[b]	Selectivity index[c]
1a	H	Cl	>100	1.86 ± 0.029	0.02
1b	CH_3	Cl	>100	72.02 ± 0.058	0.72
1c	C_2H_5	Cl	>100	>100	–
1d	OCH_3	Cl	>100	>100	–
1e	OC_2H_5	Cl	>100	>100	–
1f	F	Cl	>100	>100	–
1g	Cl	Cl	>100	>100	–
1h	Br	Cl	>100	>100	–
2a	H	Cl	1.51 ± 0.121	>100	62.11
2b	CH_3	Cl	87.09 ± 0.011	11.22 ± 0.021	0.12
2c	C_2H_5	Cl	26.30 ± 0.045	35.48 ± 0.24	1.35
2d	OCH_3	Cl	>100	>100	–
2e	OC_2H_5	Cl	>100	>100	–
2f	F	Cl	2.47 ± 0.18	>100	40.48
2g	Cl	Cl	8.31 ± 0.154	7.07 ± 0.065	0.85
2h	Br	Cl	5.49 ± 0.32	>100	18.21
Neostigmin			6.76 ± 0.012	14.45 ± 0.015	2.13
Ambenonium			4.07 ± 0.068	6.02 ± 0.045	1.48

[a]50% inhibitory concentration (means ± SD of three experiments) of AChE.
[b]50% inhibitory concentration (means ± SD of three experiments) of BuChE.
[c]Selectivity for AChE = IC50 (BuChE)/IC50 (AChE).

The target compounds (**1a–h** and **2a–h**) were synthesized using different *para*-substituted anilines with varying electronic properties. The target compounds **2f–h** were found to be effective inhibitors against AChE, which have various electron-drawing halogen groups (F, Cl and Br) at the *para*-position of the phenyl ring. To support this approach, as shown in Table 1, **2b–d** possessing an electron-donating group (–CH_3, –C_2H_5, –OCH_3, –OC_2H_5) at the *para*-position of the aniline ring moiety showed a decreased AChE inhibitory activity. These results imply that an electron-drawing group at the *para*-position of the aniline ring is beneficial to AChE inhibitory activity.

Docking simulation

To explore the possible interaction mode of the most potent compounds with AChE and BuChE, molecular modelling simulations were performed between the most active compounds, **2a** with AChE and **1a** with BuChE, using SYBYL X 2.0 Surflex-Dock software. The enzyme structures were obtained from the Protein Data Bank. The docking results showed that compound **2a** displayed multiple binding patterns with Torpedo californica (TcAChE-1ACJ), as shown in Figure 1. In the 1ACJ-**2a** complex, the oxygen atom from the carbonyl group created two hydrogen bonds with an OH group of Ser200 (2.54 Å) and an NH group of Gly118 (2.16 Å) CAS. The chloro group in the *para*-positions on benzyl rings created an H-bond, such as the OH group of Tyr334 (2.55 Å) into the PAS. The benzyl moiety of compound **2a** was

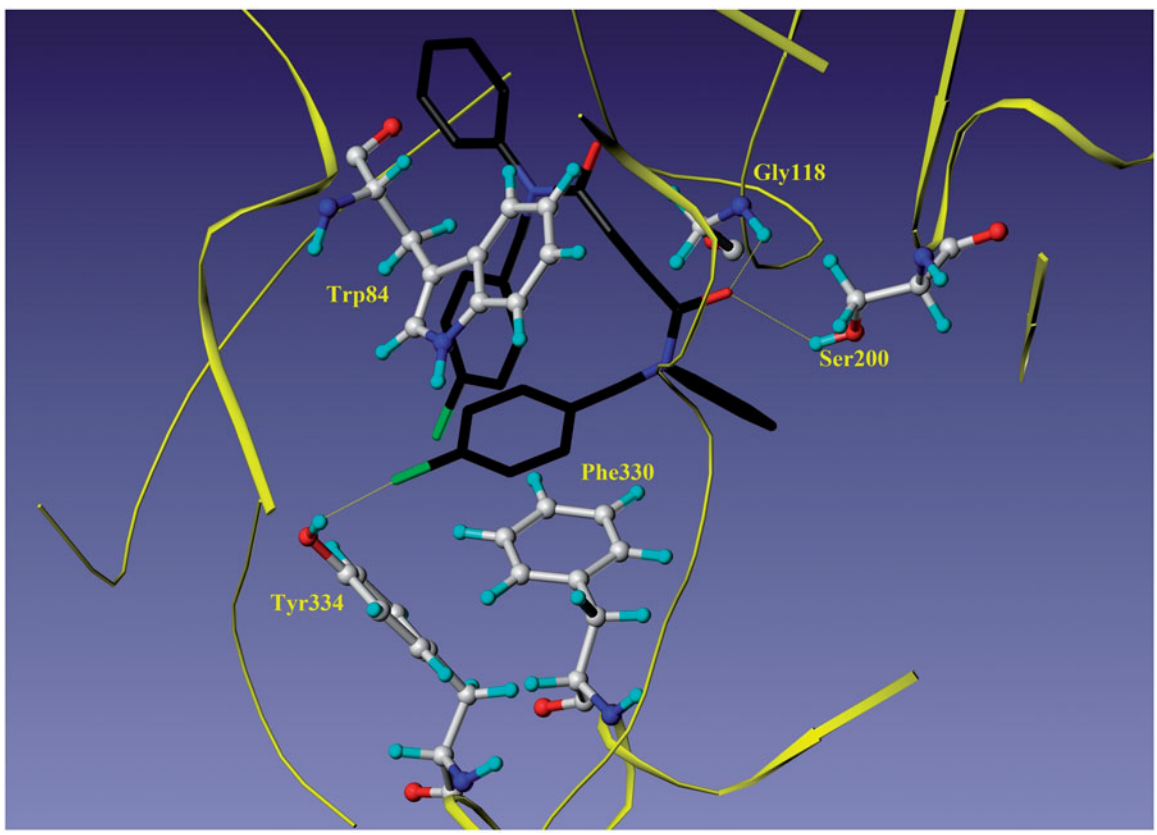

Figure 1. Docking model of compound **2a** and TcAChE complex.

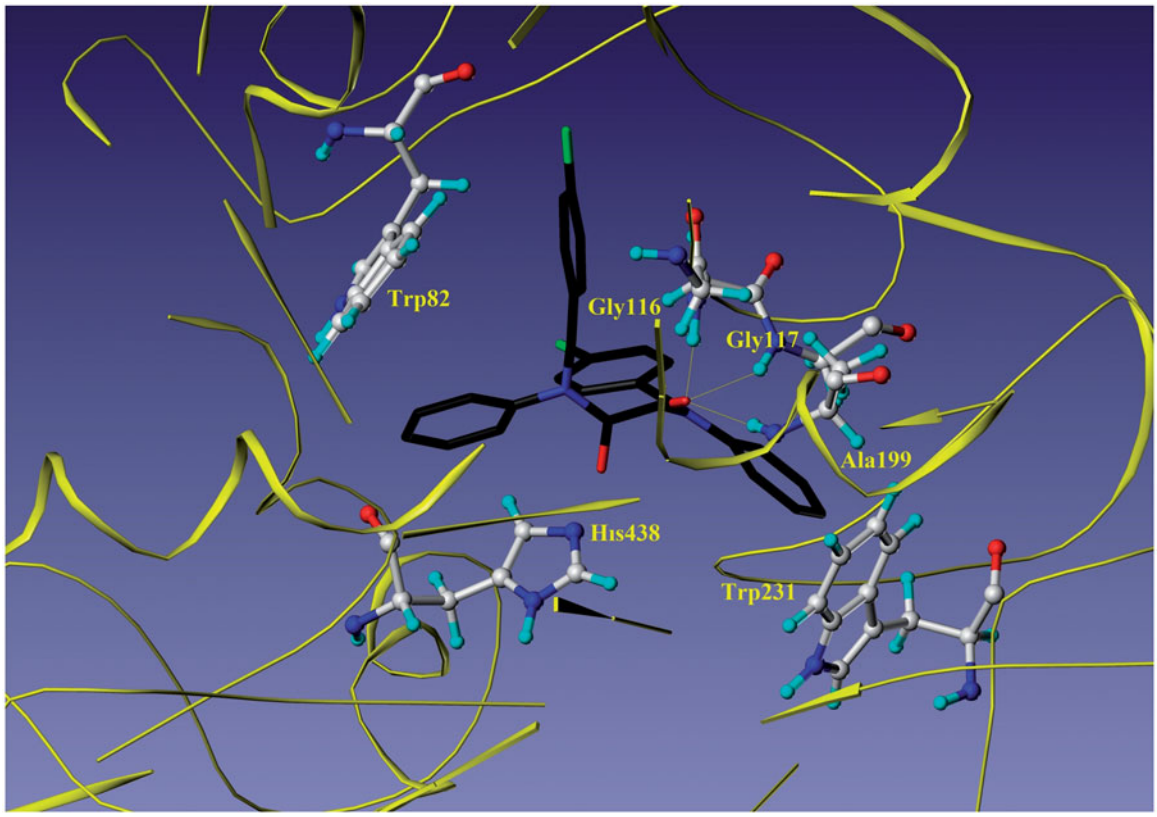

Figure 2. Docking model of compound **1a** and HuBuChE complex.

Figure 3. (a) UV spectrum of compound **1a** (100 μM). (b) Spectrum of a mixture of **1a** (100 μM) and $ZnSO_4$ (100 μM). (c) Spectrum of a mixture of **1a** (100 μM) and $CuSO_4$. (d) Spectrum of a mixture of **1a** (100 μM) and $FeSO_4$ (100 μM).

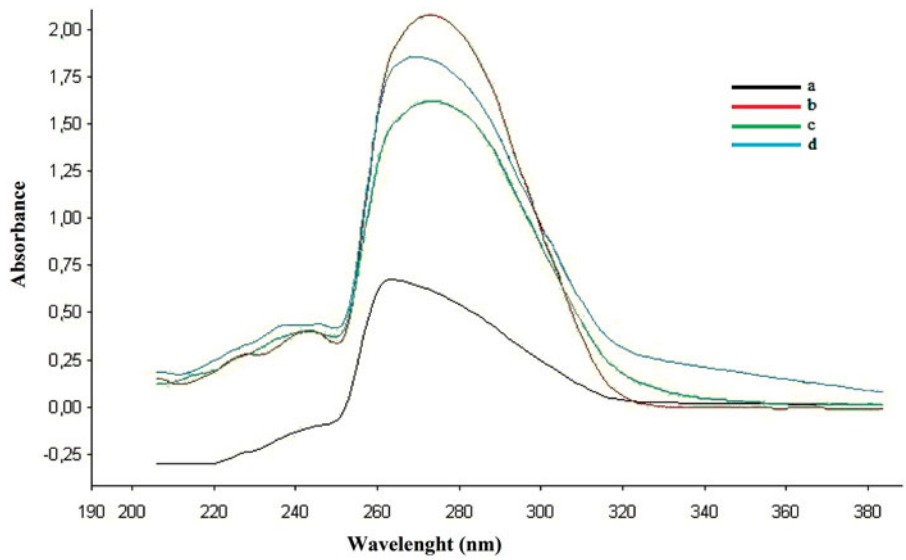

located on the residues of Trp84 and Phe330 in a ''sandwich'' form. The *p*-chlorobenzyl moiety of **2a** was observed to bind to CAS via parallel π–π stacking interactions between Trp84 (3.75 Å) and Phe330 (3.23 Å) in a ''sandwich'' form.

The most potent BuChE inhibitor, **1a**, showed interactions with Gly116, Gly117, Ala199 and Trp82 residues of human butyrylcholinesterase enzyme (HuBuChE-1P0I) (Figure 2). Hydrogen bond interactions occurred between the carbonyl group of compound **1a** and the NH groups of Gly116 (1.92 Å), Gly117 (2.06 Å) and Ala199 (2.51 Å) in an oxyanion hole of the CAS of HuBuChE. In addition, one of the phenyl rings entered the PAS of BuChE and π–π stacking interactions occurred with the indole moiety of Trp82 (3.30–5.25 Å).

Metal chelating effect

The complexation abilities of the most potent compounds, **1a** and **2a**, for metals such as Cu^{2+}, Fe^{2+} and Zn^{2+} in DMSO were studied using a UV–visible spectrophotometer. The UV absorption of the compounds in DMSO changed with the titration of Cu^{2+}, Fe^{2+} and Zn^{2+}, and the results are shown in Figures 3 and 4. The absorption peaks of compounds **1a** and **2a** in DMSO increased after the addition of Cu^{2+} and Fe^{2+}. Only compound **1a** showed an increased absorption peak after adding $ZnSO_4$. A change in the absorption intensity was observed after adding $CuSO_4$, $FeSO_4$ and $ZnSO_4$, indicating the formation of all biometal complexes for compound **1a** (Cu^{2+}, Fe^{2+} and Zn^{2+}).

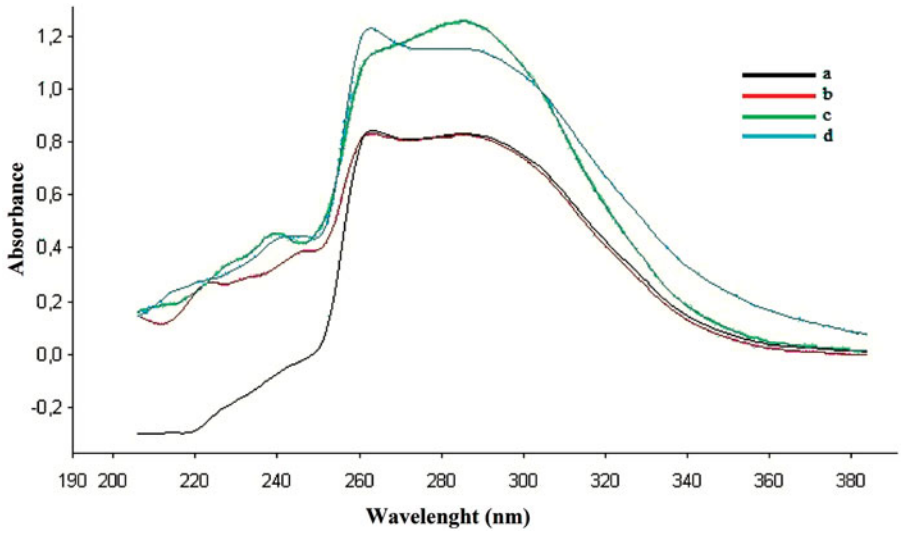

Figure 4. (a) UV spectrum of compound **2a** (100 μM). (b) Spectrum of a mixture of **2a** (100 μM) and $ZnSO_4$ (100 μM). (c) Spectrum of a mixture of **2a** (100 μM) and $CuSO_4$. (d) Spectrum of a mixture of **2a** (100 μM) and $FeSO_4$ (100 μM).

Conclusion

In conclusion, our study involved the synthesis of new oxalamide and 2-butenediamide compounds. These compounds were evaluated as potential inhibitors of ChE and as chelators of biometals. Among the synthesized 2-butenediamide derivatives, compound **2a** exhibited the greatest inhibitory potency towards AChE (IC_{50} value: 1.51 μM) and good Fe^{2+} and Cu^{2+} chelating ability. In addition, the most potent oxalamide derivative, compound **1a**, showed inhibitory activity towards BuChE (IC_{50} value: 1.86 μM). In addition, compound **1a** exhibited high-metal chelation ability with all of the biometals. Docking simulations showed that compounds **1a** and **2a** were bound mainly with the catalytic active sites of AChE and BuChE, respectively. Modelled derivatives created lots of hydrogen bonding interactions with the CAS and π–π stacking interactions with the PAS of both ChEs, which confirms their high-inhibitory potency. As a result, further investigations of AD candidates based on these results are in progress.

Declaration of interest

This research work was supported by Ataturk University Research Fund (Project No: 2013/271), Turkey. The authors have declared no conflicts of interest with the presented data from this article.

References

1. Lambert J, Heath S, Even G, et al. Genome-wide association study identifies variants at CLU and CR1 associated with Alzheimer's disease. Nat Genet 2009;41:1094–9.
2. Naj AC, Jun G, Beecham GW, et al. Common variants at MS4A4/MS4A6E, CD2AP, CD33 and EPHA1 are associated with late-onset Alzheimer's disease. Nat Genet 2011;43:436–41.
3. Piazzi L, Rampa A, Bisi A, et al. Extensive SAR and computational studies of 3-{4-[(benzylmethylamino)methyl]phenyl}-6,7-dimethoxy-2H-2-chromenone (AP2238) derivatives. J Med Chem 2003;46:2279–82.
4. Seshadri S, Fitzpatrick AL, Ikram MA, et al. Genome-wide analysis of genetic loci associated with Alzheimer disease. J Am Med Assoc 2010;303:1832–40.
5. Singh M, Kaur M, Kukreja H, et al. Acetylcholinesterase inhibitors as Alzheimer therapy: from nerve toxins to neuroprotection. Eur J Med Chem 2013;70:165–88.
6. Massoud F, Léger G. Pharmacological treatment of Alzheimer disease. Can J Psychiatry 2011;56:579–88.
7. Winslow B, Onysko M, Stob C, Hazlewood K. Treatment of Alzheimer disease. Am Fam Physician 2011;83:1403–12.
8. Akasofu S, Kimura M, Kosasa I, et al. Study of neuroprotection of donepezil, a therapy for Alzheimer's disease. Chem Biol Interact 2008;175:222–6.
9. Dumas JA, Newhouse PA. The cholinergic hypothesis of cognitive aging revisited again: cholinergic functional compensation. Pharmacol Biochem Behav 2011;99:254–61.
10. Tai HC, Serrano-Pozo A, Hashimoto T, et al. The synaptic accumulation of hyperphosphorylated tauoligomers in Alzheimer disease is associated with dysfunction of the ubiquitin-proteasome system. Am J Pathol 2012;181:1426–35.
11. Skrzypek A, Matysiak J, Niewiadomy A, et al. Synthesis and biological evaluation of 1,3,4-thiadiazole analogues as novel AChE and BuChE inhibitors. Eur J Med Chem 2013;62:311–19.
12. Darvesh S, Hopkins DA, Geula C. Neurobiology of butyrylcholinesterase. Nat Rev Neurosci 2003;4:131–8.
13. Greig NH, Utsuki T, Ingram DK, et al. Selective butyrylcholinesterase inhibition elevates brain acetylcholine, augments learning and lowers Alzheimer beta-amyloid peptide in rodent. Proc Natl Acad Sci USA 2005;102:17213–18.
14. Bullock R, Lane R. Executive dyscontrol in dementia, with emphasis on subcortical pathology and the role of butyrylcholinesterase. Curr Alzheimer Res 2007;4:277–93.
15. Jhee SS, Shiovitz T, Hartman RD, et al. Centrally acting antiemetics mitigate nausea and vomiting in patients with Alzheimer's disease who receive rivastigmine. Clin Neuropharmacol 2002;25:122–3.
16. Kamal MA, Klein P, Luo W, et al. Kinetics of human serum butyrylcholinesterase inhibition by a novel experimental Alzheimer therapeutic, dihydrobenzodioxepine cymserine. Neurochem Res 2008;33:745–53.
17. Mesulam MM, Guillozet A, Show P, et al. Acetylcholinesterase knockouts establish central cholinergic pathways and can use butyrylcholinesterase to hydrolyze acetylcholine. Neuroscience 2002;110:627–39.
18. Basiri A, Murugaiyaha V, Osman H, et al. An expedient, ionic liquid mediated multi-component synthesis of novel piperidone grafted cholinesterase enzymes inhibitors and their molecular modeling study. Eur J Med Chem 2013;67:221–9.
19. Khoobi M, Alipour M, Moradi A, et al. Design, synthesis, docking study and biological evaluation of some novel tetrahydrochromeno [3′,4′:5,6]pyrano[2,3-b]quinolin-6(7H)-one derivatives against acetyl- and butyrylcholinesterase. Eur J Med Chem 2013;68:291–300.
20. Budimir A. Metal ions, Alzheimer's disease and chelation therapy. Acta Pharm 2011;61:1–14.
21. Liu G, Huang W, Moir RD, et al. Metal exposure and Alzheimer's pathogenesis. J Struct Biol 2006;155:45–51.
22. Zatta P, Drago D, Bolognin S, Sensi SL. Alzheimer's disease, metal ions andmetal homeostatic therapy. Trends Pharmacol Sci 2009;30:346–55.
23. Loef M, Walach H. Copper and iron in Alzheimer's disease: a review and its dietary implications. Br J Nutr 2012;107:7–19.

24. Dong J, Atwood CS, Anderson VE, et al. Metal binding and oxidation of amyloid-beta within isolated senile plaque cores: Raman microscopic evidence. Biochemistry 2003;42:2768–73.
25. Opazo C, Huang X, Cherny RA, et al. Cu-dependent catalytic conversion of dopamine, cholesterol, and biological reducing agents to neurotoxic H(2)O(2). J Biol Chem 2002;277:40302–8.
26. Yan H, Yao PF, Chen SB, et al. Synthesis and evaluation of 7,8-dehydrorutaecarpine derivatives as potential multifunctional agents for the treatment of Alzheimer's disease. Eur J Med Chem 2013;63:299–312.
27. Ellman GL, Courtney D, Andies V, Featherstone RM. A new and rapid colorimetric determination of acetylcholinesterase activity. Biochem Pharmacol 1961;7:88–95.
28. Musileka K, Komloova M, Holas O, et al. Preparation and *in vitro* screening of symmetrical bis-isoquinolinium cholinesterase inhibitors bearing various connecting linkage – implications for early Myasthenia gravis treatment. Eur J Med Chem 2011;46:811–18.
29. Huang W, Lv D, Yu H, et al. Dual-target-directed 1,3-diphenylurea derivatives: BACE 1 inhibitor and metal chelator against Alzheimer's disease. Bioorg Med Chem 2010;18:5610–15.
30. Joseph R, Ramanujam B, Acharya A, et al. Experimental and computational studies of selective recognition of Hg^{2+} by amide linked lower rim 1,3-dibenzimidazole derivative of calix[4]arene: species characterization in solution and that in the isolated complex, including the delineation of the nanostructures. J Org Chem 2008;73:5745–58.
31. Yerdelen KO, Gul HI. Synthesis and anticholinesterase activity of fumaramide derivatives. Med Chem Res 2013;22:4920–9.

Supplementary material available online